Available online at www.sciencedirect.com
ScienceDirect
Journal of Photochemistry and Photobiology A: Chemistry 192 (2007) 1–7
Journal of Photochemistry and Photobiology A:Chemistry
www.elsevier.com/locate/jphotochem

Electroluminescence from organic/inorganic heterostructure device based on blends of PVK and water–sol CdSe nanocrystals

A.W. Tang, F. Teng *, S. Xiong, Y.H. Gao, C.J. Liang, Y.B. Hou *

Key laboratory of Luminescence and Optical Information, Ministry of Education, Institute of Optoelectronic Technology, Beijing JiaoTong University, Beijing 100044, China

Received 15 January 2007; received in revised form 11 March 2007; accepted 30 April 2007
Available online 3 May 2007

Abstract

Organic/inorganic heterostructure devices were fabricated with polymer material poly(*N*-vinylcarbazole) (PVK) and CdSe nanocrystals synthesized in aqueous solution. Stable electroluminescence (EL) was obtained from the organic/inorganic heterostructure devices with different mass ratios of CdSe to PVK and under different applied voltages. With increasing applied voltages, the ratio of EL from CdSe nanocrystals to that from PVK decreased, and the color of the emission could be tuned from yellow to white. By changing the mass ratios of CdSe to PVK and the applied voltages, we obtained a pure white color from the heterostructure device with the CIE coordinates of (0.313, 0.336) for the mass ratio of CdSe:PVK = 9:1 at 24 V. The EL emission from the devices is mainly attributed to the incomplete energy transfer and carrier trapping directly on CdSe nanocrystals.

Keywords: Electroluminescence; CdSe nanocrystals; Organic/inorganic; Poly(*N*-vinylcarbazole)

1. Introduction

During the past several decades, organic light-emitting diodes (OLEDs) based on conjugated polymers have attracted much attention due to their excellent performance for panel displays [1–3]. Great efforts have been devoted to improving the performance of OLEDs by increasing their efficiency, narrowing or broadening their emission spectra, or polarizing their emission. Recently, some studies of organic/inorganic heterostructure devices based on semiconductor nanocrystals (such as CdSe, CdTe) and polymer materials have been widely reported [4–10]. As a new type of optical materials, semiconductor nanocrystals have presented their unique luminescence characteristics, such as size-dependent color variation and high photoluminescence quantum yield [10–14]. These advantages make nanocrystals as an ideal candidate in a wide range of the potential applications, such as applications in LEDs and photovoltaic devices [15–20]. These organic/inorganic heterostructure devices combine the diversity of polymer materials with good electronic and optical properties of semiconductor nanocrystals. Especially, in recent years, some groups have obtained white light emission by mixing polymer and semiconductor nanocrystals [21–23]. Ma and co-workers attributed the realization of white light emission to the incomplete energy and charge transfer from polymer to semiconductor nanocrystals [22]. Although much progress in the organic/inorganic heterostructure devices has been made in the past few years, yet the semiconductor nanocrystals used in such devices were synthesized by a wet chemical route together with the non-aqueous trioctyl phosphine/trioctyl phosphine oxide (TOP/TOPO) systems [15–22]. However, not only is the method complicated but also the TOPO/TOP systems are toxic and expensive. More importantly, the nanocrystals synthesized by this method have a TOPO passivation layer, which is larger than the alkyl chain capped on the functionalized water–sol nanocrystals and probably makes injection of carriers into the nanocrystals more difficult. Unfortunately, it is difficult for water–sol nanocrystals to be imported into organic solvents to mix with polymers. Recently, Yang's group has successively used surfactants to transfer water–sol CdTe nanocrystals into fluorescent nanocrystal-polymer transparent composites via electrostatic interaction, which is an alternative

* Corresponding authors. Tel.: +86 10 51688605; fax: +86 10 51683933.
E-mail addresses: fteng@bjtu.edu.cn (F. Teng), ybhou@bjtu.edu.cn (Y.B. Hou).

1010-6030/$ – see front matter © 2007 Elsevier B.V. All rights reserved.
doi:10.1016/j.jphotochem.2007.04.029

route to disperse water–sol nanocrystals into different types of polymers [24,25].

In this paper, CdSe nanocrystals were synthesized in aqueous solution by a traditional method and were transferred from aqueous solution into chloroform via a surfactant cetyltrimethyl ammonium bromide (CTAB). Organic/inorganic heterostructure devices were fabricated with blends of CdSe nanocrystals and PVK, which were used as an emissive layer. The dependence of EL efficiency and current–voltage characteristics on the mass ratios of CdSe nanocrystals to PVK was investigated, and the result shows that the current efficiency is comparable with that of the nanocrystal-polymer device by using the nanocrystals capped by a TOPO layer [19,20]. At the same time, a pure white light emission with CIE coordinates of (0.313, 0.336) was obtained at 24 V when the mass ratio of CdSe to PVK was 9:1.

2. Experimental

2.1. Synthesis of CdSe nanocrystals

The synthesis method of CdSe nanocrystals was based on a previous reference [26]: the pH value of an aqueous solution of $Cd(CH_3COO)_2{\cdot}2H_2O$ and 2-mercaptoacetic acid was adjusted to 10–11 by using sodium hydroxide, following by addition of an aqueous solution of Na_2SeSO_3 under vigorous stirring at N_2 atmosphere. Then the solution was heated to 80 °C and refluxed for several hours to promote the growth of CdSe nanocrystals. The resulting CdSe nanocrystals were redispersed in the aqueous solution and a surfactant (CTAB) was used to transfer them from the aqueous solution to chloroform solution.

2.2. Device fabrication

A thin hole injection layer of poly(3,4-ethylenedioxythiophene):poly(styrenesulfonate) (PEDOT:PSS) with a thickness of 50–60 nm was spin-coated onto a cleaned Indium-tin-oxide (ITO) glass substrates and the layer then was heated to 80 °C for about 10 min. The PEDOT:PSS layer was used to improve the holes transport [16]. Then the blends of CdSe nanocrystals and PVK were spin-coated from chloroform solution onto the top of PEDOT:PSS layer, and the mass ratios of CdSe:PVK were 2:1, 5:1 and 9:1, respectively, which are denoted as film A, B and C. The thickness of the layer was about 60–80 nm. The organic films of Bathocuproine (BCP) (10 nm) and Aluminum tris(8-hydroxyquinoline) (Alq_3) (10 nm) were vapor-deposited onto the nanocomposite layer successively by the thermal evaporation method. Herein, BCP and Alq_3 were used as the hole-blocking layer and the electron-transporting layer, respectively. Finally, the cathode of Al was used as the top electrode. Accordingly, the devices are denoted as devices A–C.

3. Results and discussion

The X-ray powder diffraction (XRD) pattern of CdSe nanocrystals is shown in Fig. 1a, which gives a broad peak typical for nanocrystals. The positions of all the diffraction peaks match well with those from JCPDS card (19–091) and indicate the as-prepared CdSe nanocrystals in cubic phase [27]. Fig. 1b presents the X-ray photoelectron spectra (XPS) analysis results of CdSe nanocrystals. The peaks at 405.0 and 412.0 eV correspond to the binding energy of $Cd3d_{5/2}$ and $Cd3d_{3/2}$ and the peak at 54.2 eV corresponds to the binding energy of Se3d, which confirm the existence of cadmium and selenium species in the nanocrystals. These results indicate the formation of CdSe nanocrystals [28]. The transmission electron microscopy (TEM) image of CdSe nanocrystals is shown in Fig. 1c. This image clearly displays

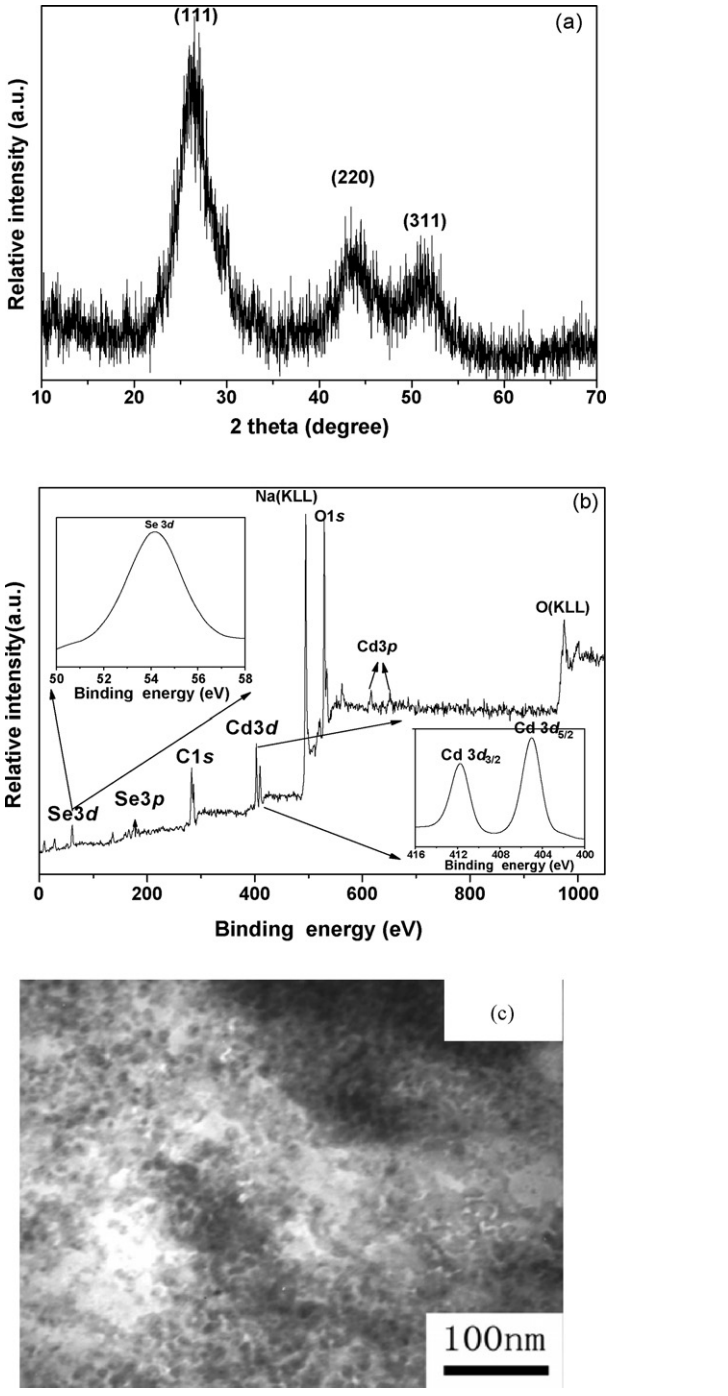

Fig. 1. (a) XRD pattern of CdSe nanocrystals; (b) XPS spectra of CdSe nanocrystals. The insets are the expanded spectra of Cd 3d and Se 3d. (c) TEM image of CdSe nanocrystals.

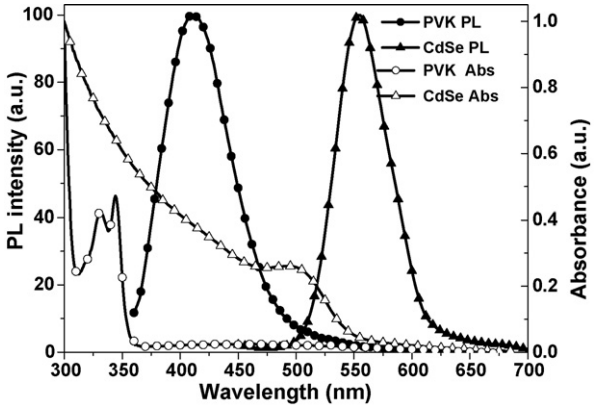

Fig. 2. Normalized absorption spectra of CdSe nanocrystals (dashed line) and PVK (dotted line), and PL spectra of CdSe nanocrystals (dash doted line, λ_{ex} = 420 nm) and PVK (solid line, λ_{ex} = 330 nm).

the nearly spherical shape of the particles and the size of the particles is less than 10 nm.

Fig. 2 shows the normalized absorption and photoluminescence (PL) spectra of CdSe nanocrystals in chloroform and PVK film on a quartz substrate. The relative photoluminescence quantum yields of CdSe nanocrystals in chloroform and in aqueous solution are estimated to be about 9% and 8%, respectively, using Rhodamine B in ethanol as a standard. According to the theory of Förster energy transfer, the rate of the energy transfer and Förster radius can be given in the following expressions:

$$k_{\text{Förster}} = \tau_{\text{d}}^{-1}\left(\frac{R_0}{r}\right)^6,$$

$$R_0^6 = \alpha \int F_{\text{d}}(\nu)\varepsilon_{\text{a}}(\nu)\nu^{-4}\,\text{d}\nu$$

where τ_{d} is the lifetime of the donor in the absence of the acceptor, r is the distance between the donor and acceptor, R_0 is the Förster radius, and $F_{\text{d}}(\nu)$ and $\varepsilon_{\text{a}}(\nu)$ are the fluorescence and extinction spectra of the donor and acceptor, respectively. From the expression, we can deduce that the necessary condition of Förster energy transfer is the spectral overlap between the emission of the donor and the absorption of the acceptor and a maximum distance between the two constituents of 3–5 nm [20]. The two conditions are verified in the CdSe:PVK blend system. In such systems, both PVK and CdSe are mixed together but not spacially separated, and a clear spectral overlap between the emission of PVK and the absorption of CdSe nanocrystals is observed in Fig. 2. Therefore, the Förster energy transfer from PVK to CdSe nanocrystals can be expected to occur [21]. To further confirm the existence of the energy transfer from PVK to CdSe, we measured the photoluminescence lifetimes of PVK and CdSe:PVK films measured at the wavelength of 410 nm. The photoluminescence lifetimes of PVK and CdSe:PVK thin films obtained from the multi-exponential decay are listed in Table 1. The average photoluminescence lifetime of CdSe:PVK film is about 7.61 ns, which is shorter than that of PVK film (12.5 ns). This result indicates the existence of the energy transfer from PVK to CdSe naocrystals [29,30].

Table 1
Photoluminescence intensity decay properties of PVK and CdSe:PVK thin films

Sample	τ_1 (ns) (α_1%)	τ_2 (ns) (α_2%)	τ_3 (ns) (α_3%)	τ (ns)
PVK	16.9 (41.19%)	4.19 (52.53%)	53.6 (6.28%)	12.5
CdSe:PVK	12.33 (32.54%)	2.41 (64.80%)	76.6 (2.66%)	7.61

τ is the average decay time calculated from $(\sum_i^3 \tau_i\alpha_i)/100$. τ_i and α_i are the fluorescence lifetime and the percentage of multi-exponential decay [28].

The normalized PL spectra of CdSe:PVK films with different mass ratios of CdSe to PVK are shown in Fig. 3. In these spectra, the emission peak at 575 nm is attributed to the exciton formation in CdSe nanocrystals and the emission band at 410 nm is attributed to the relaxation of excited dimmers formed between neighboring carbazole groups in PVK. It reveals that the intensity of the emission from PVK is stronger than that from CdSe nanocrystals under the excitation wavelength of 330 nm, suggesting that the energy transfer from PVK to CdSe nanocrystals is incomplete [22]. At the same time, the relative intensity of the emission from CdSe is enhanced as the mass ratio of CdSe to PVK varies from 1:2 to 2:1 but decreases when the mass ratio of CdSe to PVK is higher than 2:1. If the energy transfer from PVK to CdSe nanocrystals is complete, the relative intensity of the emission from the nanocrystals would be much stronger than that from PVK. However, the relative intensity of the emission from CdSe is relatively weak as compared with that from PVK. It is considered that the emission from CdSe nanocrystals originates from not only the Förster energy transfer from the polymer to the nanocrystals but also the direct excitation of 330 nm incident light which is propitious to the excitation of PVK. The intensity of CdSe nanocrystals is strongest of all when the mass ratio of CdSe to PVK is 2:1, which may be attributed to the following reasons: (1) when the concentration of CdSe in nanocomposites is too high, the aggregation of the nanocrystals will occur which will result in the concentration quenching and influence the PL efficiency of CdSe nanocrystals; (2) the energy transfer is most efficient for this mass ratio because CdSe nanocrystals can be modified successfully and the dispersion of CdSe nanocrystals in PVK is well unified. As to the genuine rea-

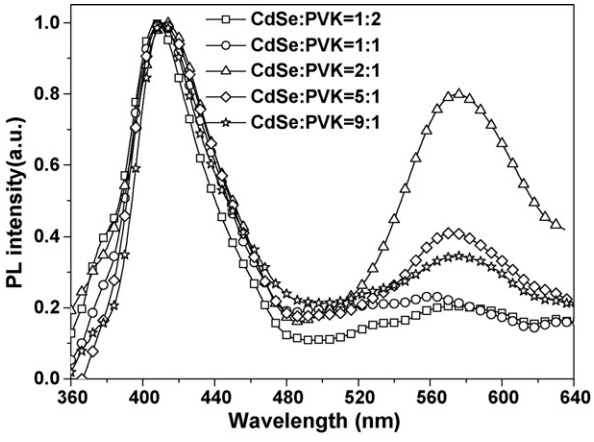

Fig. 3. Normalized PL spectra of CdSe:PVK composite films with different mass ratios of CdSe to PVK (λ_{ex} = 330 nm).

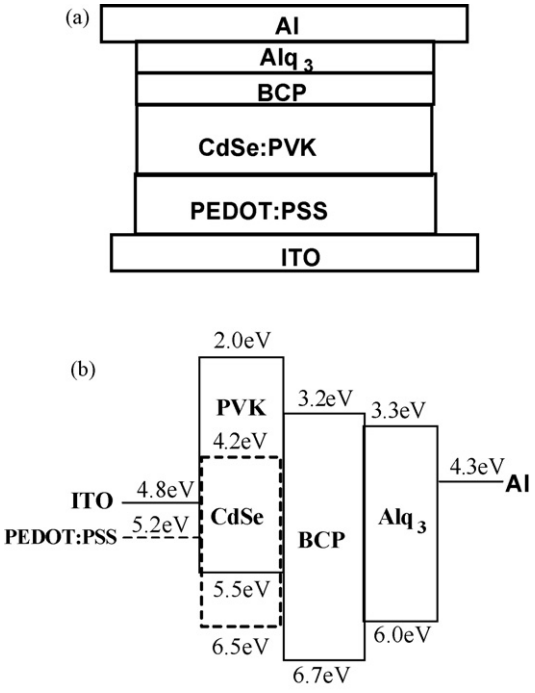

Fig. 4. (a) Device configuration and (b) the energy level diagram of the heterostructure device.

son, however, it will be investigated in detail in the future work.

The device configuration and the energy level diagram of the heterostructure device are shown in Fig. 4. The electronic energy levels of ITO, PEDOT:PSS, Al electrodes, BCP, Alq_3 and CdSe nanocrystals are taken from previous experimental data [31–33]. In the heterostructure device, holes are considered to be injected from the ITO electrode through PEDOT:PSS layer into the PVK hole conductor layer and be accumulated at the interface of the nanocrystal layer. Similarly, electrons are considered to be injected from Al electrode through the electron-transporting layer Alq_3 into BCP and arrive at the CdSe:PVK/BCP interface.

Fig. 5a shows the normalized EL spectra of device A under different applied voltages and the normalized PL spectrum of the composite film A. It is clearly observed that the electroluminescence from the device is dominated by the emission from the nanocrsytals and the intensity of the emission from PVK is relatively weak. However, the intensity of the emission from PVK is enhanced but that from the nanocrystals is restrained in the PL spectrum of the composite film. This can be attributed to the difference between the PL process and EL process, and the reasons can be summarised as follows: in the EL process, the electroluminescence is generated by either direct injection of holes and electrons into the nanocrystals or by the Förster energy transfer of excitons onto the nanocrystals from PVK, which has been reported in previous references [5,23]. When the heterostructure device is excited under the electric field, the direct injection of electrons into the nanocrystals is enhanced greatly. This is because CdSe is mainly as an electron trap (Fig. 4b), which can seize an electron firstly and absorb a hole through the Coulomb force, and then the holes and the electrons can be efficiently delivered to the active layers of the devices to create

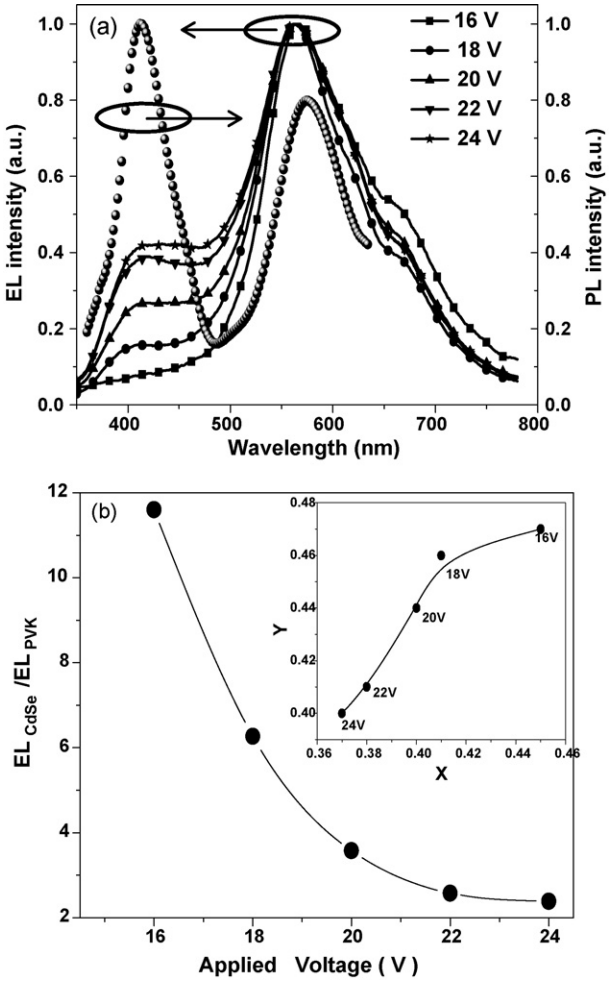

Fig. 5. (a) Normalized EL spectra of device A under different applied voltages and normalized PL spectrum of the thin film A. (b) Voltage dependence on the ratio of CdSe nanocrystals EL to PVK EL for device A, the inset shows the CIE coordinates vs. applied voltages for device A.

excitons, which recombine in the nanocrystals [34]. Alternatively, the excitons can also undergo Förster energy transfer from PVK to the lower-energy CdSe nanocrystals sites. In the PL process, however, the excitation light energy is mainly absorbed by PVK and the excitons are formed in PVK. Subsequently, some excitons take part in the direct radiation recombination luminescence, and then the energy of the other excitons is transferred to CdSe nanocrystals by incomplete energy transfer, resulting in the luminescence of CdSe nanocrystals. Therefore, the intensity of the emission from CdSe nanocrystals is relative weak as compared with that from PVK. In addition, we observe that the there is little change of the peaks positions in the PL and EL spectra of the composite film, and the full width at half maximum (FWHM) of EL spectra becomes broader than that of PL spectra. This indicates that the origin of the EL of the device is mainly from the CdSe:PVK composite film, and the device structure and the surface coverage of the composite film are directly related to the EL emission from the devices. It is also found in Fig. 5a that the intensity of the emission from PVK increases with increasing applied voltages. In order to study the influence of the applied voltages on the emission from CdSe nanocrystals and that from

PVK, the EL spectra of device A were fitted with Gaussians to obtain the individual peak. We have compared the ratio of integrated intensity of CdSe nanocrystals to that of PVK under different applied voltages. The results show that the ratio of the EL from CdSe nanocrystals to that from PVK decreases significantly as the applied voltage changes from 16 to 24 V (Fig. 5b). This behavior may be attributed to the fact that PVK and CdSe nanocrystals are drastically different materials with disparate dielectric constants and transport mechanisms, which makes the recombination zone move with the applied voltage. Such similar results are also observed in Alivisatos's reports [4,15]. On the other hand, because the energy difference between the LUMO of PVK and the conduction band of CdSe is larger than the difference between the HOMO and valence band (Fig. 4b), the difference favors injection of holes into nanocrystals over electrons into PVK. However, the charge gradient and the voltage drop across the junction are larger under higher applied voltages. This forces migration of a higher fraction of electrons into the hole-transporting layer PVK at higher applied voltages, resulting in a PVK contribution to the EL spectra of the device [8]. The CIE coordinates of the device ranges from (0.45, 0.47) to (0.37, 0.40) when the applied voltage varies from 16 to 24 V (inset of Fig. 5b). According to 1931 CIE Chromaticity Diagram, the coordinates of (0.45, 0.47) is in the range of yellow-light region and the coordinates of (0.37, 0.40) is in the range of white-light region, respectively. This indicates that the color of the emission from the device changes from yellow to white by changing the applied voltages. Furthermore, it is more interesting that there is a shoulder peak centered at 665 nm in the EL spectra of device A. This peak can probably result from electroplex emission at CdSe:PVK/BCP interface according to the emission peak and the device structure. At present, however, the genuine reason has not been distinguished clearly.

Fig. 6a gives the EL spectra of devices A–C at the same applied voltage of 24 V. It is found that the EL intensity increases obviously as the mass ratio of CdSe to PVK decreases, which is consistent with the results of the PL spectra of CdSe:PVK composite film. By calculation, the current efficiency of the device varies from 0.124 Cd A^{-1} for device C to 0.066 Cd A^{-1} for device A at the applied voltage of 24 V. The CIE diagram with the color coordinates for the devices is shown in Fig. 6b. It can be seen that the CIE coordinates vary from (0.373, 0.406) for device A to (0.313, 0.336) for device C, which are all located in the range of white-light region. Especially for device C, the CIE coordinates are almost overlapped the equi-energy white point (0.333, 0.333). In order to study the effect of the applied voltage on the CIE coordinates of the white emission from device C, the EL spectra of device C under the applied voltages of 16, 20 and 24 V are given in Fig. 7a. The CIE coordinates of the emission from device C change from (0.338, 0.393) at 16 V to (0.313, 0.336) at 24 V, which are also located in the white region, and the results are seen in Fig. 7b. This indicates that a pure white emission can be obtained from the heterostructure device by changing the mass ratio of CdSe to PVK and the applied voltages. The maximum current efficiency of device C is calculated to be about 0.22 Cd A^{-1} at 24 V, which is expected to be improved by optimizing the device structure, such as the use of the metals with lower work function for cathode electrode, better electron- or hole-transporting layer and the nanocrystals emitters with improved luminescence efficiency [23].

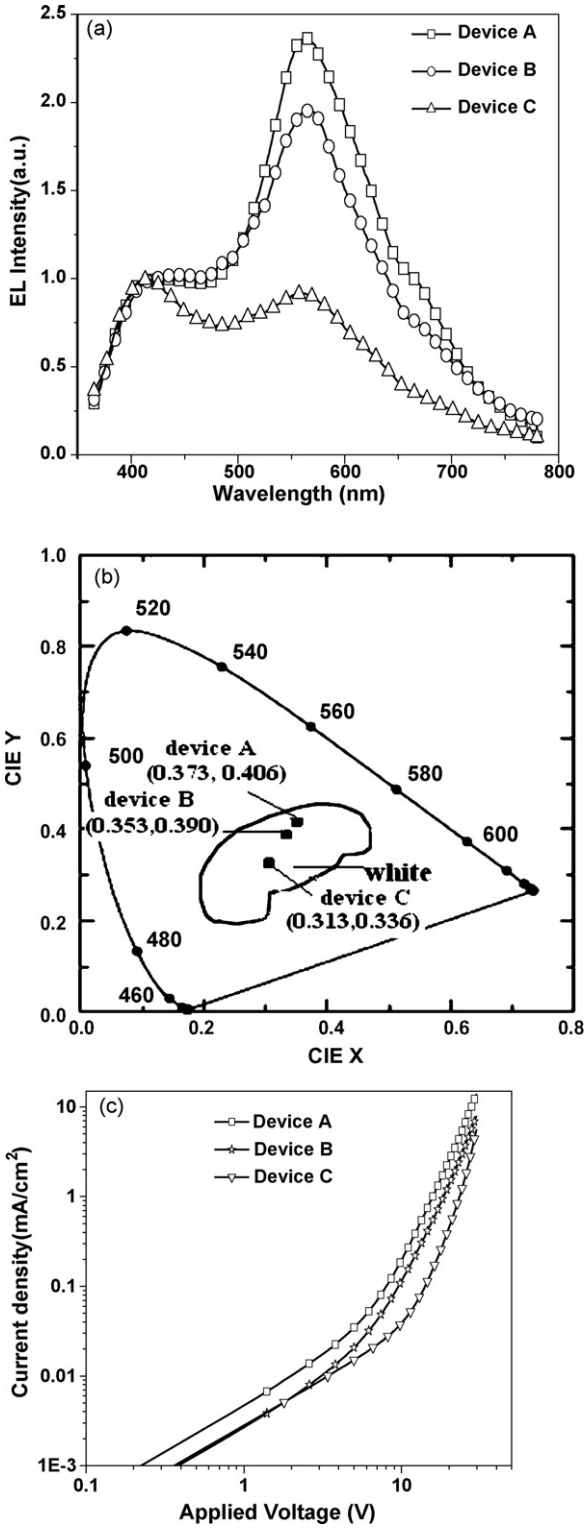

Fig. 6. (a) EL spectra under the applied voltage of 24 V, (b) CIE diagram with the color coordinates of the emitted light at 24 V for devices A–C and (c) current density–voltage characteristics of devices A–C.

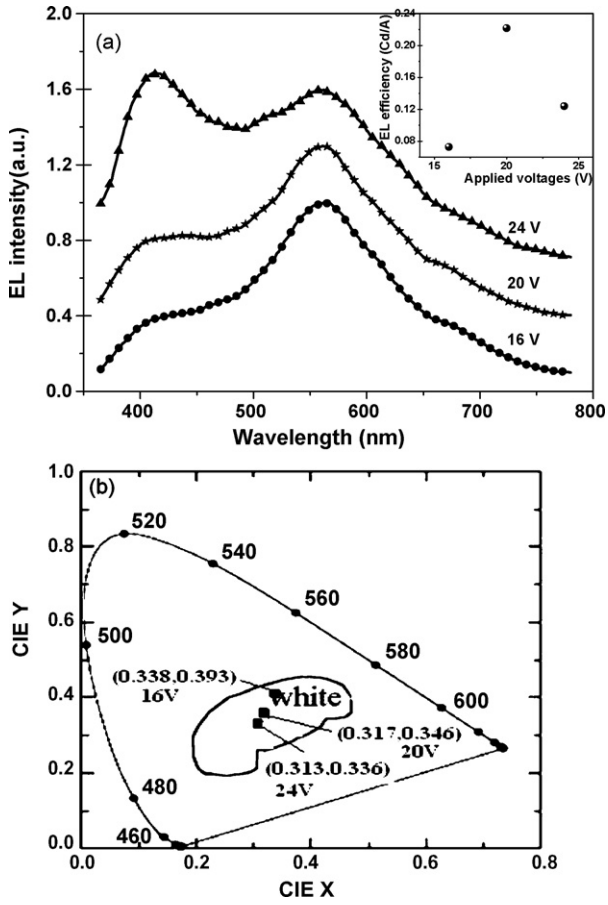

Fig. 7. (a) EL spectra of device C under the applied voltages of 16, 20 and 24 V, and the inset shows the current efficiency of device C at the corresponding voltages. (b) CIE diagram with the color coordinates of the EL emission from device C at the applied voltages of 16, 20 and 24 V.

The current density–voltage characteristics of devices A–C are shown in Fig. 6c. This display a nearly ohmic behavior at lower voltage and the current dramatically increases for higher voltages. It is seen that the turn-on voltage decreases dramatically with the decreasing of the mass ratio of CdSe to PVK. These results suggest that PVK plays a critical part for the holes injection and transportation in the device. On the other hand, because the electron mobility is higher than the holes mobility ($\mu_e/\mu_h = 8$–10) [8], which could result in a higher probability for electrons to cross the interface and reach the anode without recombination when the concentration of CdSe in the composite film is too high.

4. Conclusions

In summary, water–sol CdSe nanocrystals were incorporated into an organic/inorganic heterostructure device combining with the polymer PVK. The optoelectronic characteristics of the devices were studied based on the different applied voltages and the different mass ratios of CdSe to PVK. The ratio of the EL intensity of CdSe nanocrystals to that of PVK decreased significantly with the increasing applied voltages, and higher EL intensity and lower turn-on voltage were obtained as the mass ratios of CdSe nanocrystals to PVK decreased. By tuning the applied voltages and the mass ratios of CdSe to PVK, a pure white light emission with the CIE coordinates of (0.313, 0.336) can be obtained at 24 V from the device when the mass ratio of CdSe to PVK is 9:1. This result foreshows a simple method, which is easy to follow, to obtain white light emission from a nanocrystal-polymer lighting emitting device.

Acknowledgments

This work was supported by the National Key Project of Basic Research of China (No. 2003CB314707), National Natural Science Foundation of China (NSFC) (Nos. 90301004, 10434030 and 90401006), Key Project of Chinese Ministry of Education (No. 105041) and Beijing NOVA program (No. 2004B10). The authors thank Z. Yan and R.X. Li from DHS Instrument Co. Ltd for assistance with the fluorescence lifetime measurements.

The author (Aiwei Tang) is also grateful to the Doctor Innovation Foundation of Beijing JiaoTong University (No. 48023) for funding this research.

References

[1] C.W. Tang, S.A. VanSlyke, Appl. Phys. Lett. 51 (1987) 913.
[2] M.A. Baldo, M.E. Thompson, S.R. Rorrest, Nature 403 (2000) 750.
[3] J.K. Lee, D.S. Yoo, E.S. Handy, M.F. Rubner, Appl. Phys. Lett. 69 (1996) 1686.
[4] V.L. Colvin, M.C. Schlamp, A.P. Alivisatos, Nature 370 (1994) 354.
[5] S. Coe, W.K. Woo, M. Bawendi, V. Bulović, Nature 420 (2002) 800.
[6] M.Y. Gao, B. Richter, S. Kirstein, H. Mohwald, J. Phys. Chem. B 102 (1998) 4096.
[7] K.S. Narayan, A.G. Manoj, J. Nanda, D.D. Sarma, Appl. Phys. Lett 74 (1999) 871.
[8] H. Mattoussi, L.H. Radzilowski, B.O. Dabbousi, E.L. Thomas, M.G. Bawendi, M.F. Rubner, J. Appl. Phys. 83 (1998) 7965.
[9] M.Y. Gao, B. Richter, S. Kirstein, Adv. Mater. 9 (1997) 802.
[10] N.P. Gaponik, D.V. Talapin, A.L. Rogach, Phys. Chem. Chem. Phys. 1 (1999) 1787.
[11] X.G. Peng, M.C. Schlamp, A.V. Kadavanich, A.P. Alivisatos, J. Am. Chem. Soc. 119 (1997) 7019.
[12] Y. Tian, T. Newton, N.A. Kotov, J. Phys. Chem. B 100 (1996) 8927.
[13] Z.A. Peng, X.G. Peng, J. Am. Chem. Soc. 123 (2001) 183.
[14] M.Y. Gao, S. Kirstein, H. Mohwald, J. Phys. Chem. B 102 (1998) 8360.
[15] M.C. Schlamp, X.G. Peng, A.P. Alivisatos, J. Appl. Phys. 82 (1997) 5837.
[16] J.L. Zhao, J.Y. Zhang, C.Y. Jiang, J. Bohnenberger, T. Basché, A. Mews, J. Appl. Phys. 96 (2004) 3206.
[17] N.C. Greenham, X.G. Peng, A.P. Alivisatos, Phys. Rev. B 54 (1996) 17628.
[18] W.U. Huynh, X.G. Peng, A.P. Alivisatos, Adv. Mater. 11 (1999) 923.
[19] B.O. Dabbousi, M.G. Bawendi, O. Onitsuka, M.F. Rubner, Appl. Phys. Lett. 66 (1995) 1316.
[20] Y.Q. Li, A. Rizzo, M. Mazzeo, L. Carbone, L. Manna, R. Cingolani, G. Gigli, J. Appl. Phys. 97 (2005) 113501.
[21] P.J.H. Park, J.Y. Kim, B.D. Chin, Y.C. Kim, J.K. Kim, O.O. Park, Nanotechnology 15 (2004) 1217.
[22] Y. Xuan, D.C. Pan, N.N. Zhao, X.L. Ji, D.G. Ma, Nanotechnology 17 (2006) 4966.
[23] H.Z. Sun, J.H. Zhang, H. Zhang, Y. Xuan, C.L. Wang, M.J. Li, Y. Tian, Y. Ning, D.G. Ma, B. Yang, Z.Y. Wang, Chem. Phys. Chem. 7 (2006) 2492.
[24] H. Zhang, Z.C. Cui, Y. Wang, K. Zhang, X.L. Ji, C.L. Lv, B. Yang, M.Y. Gao, Adv. Mater. 15 (2003) 777.
[25] M.J. Li, H. Zhang, J.H. Zhang, C.L. Wang, K. Han, B. Yang, J. Colloid Interface Sci. 300 (2006) 564.

[26] S.M. Liu, H.Q. Guo, Z.H. Zhang, W. Chen, Z.G. Wang, Phys. E 8 (2000) 174.
[27] Y.J. Yang, B.J. Xiang, J. Cryst. Growth 284 (2005) 453.
[28] Y.L. Yan, Y. Li, X.F. Qian, J. Yin, Z.K. Zhu, Mater. Sci. Eng. B 103 (2003) 202.
[29] J.X. Cheng, S.H. Wang, X.Y. Li, Y.J. Yan, S.H. Yang, C.L. Yang, J.N. Wang, W.K. Ge, Chem. Phys. Lett. 333 (2001) 375.
[30] H.Y. Byun, I.J. Chung, H.K. Shim, C.Y. Kim, Chem. Phys. Lett. 393 (2004) 197.
[31] Y.M. Wang, F. Teng, Z. Xu, Y.B. Hou, Y.S. Wang, X.R. Xu, Appl. Surf. Sci. 243 (2005) 355.
[32] Y.M. Wang, F. Teng, Z. Xu, Y.B. Hou, S.Y. Yang, L. Qian, T. Zhang, D.A. Liu, Appl. Surf. Sci. 236 (2004) 251.
[33] S. Coe-Sullivan, W.-.K. Woo, J.S. Steckel, M.G. Bawendi, V. Bulović, Org. Electron. 4 (2003) 123.
[34] S. Coe-Sullivan, J.S. Steckel, W.-K. Woo, M.G. Bawendi, V. Bulović, Adv. Funct. Mater. 15 (2005) 1117.